ELSEVIER

Chemical Engineering Journal 138 (2008) 249–257

Chemical Engineering Journal

www.elsevier.com/locate/cej

Lead and copper biosorption by marine red algae *Gelidium* and algal composite material in a CSTR (“Carberry” type)

Vítor J.P. Vilar, Cidália M.S. Botelho, Rui A.R. Boaventura*

LSRE-Laboratory of Separation and Reaction Engineering, Departamento de Engenharia Química,
Faculdade de Engenharia da Universidade do Porto, Rua Dr. Roberto Frias, 4200-465 Porto, Portugal

Received 24 October 2006; received in revised form 4 July 2007; accepted 11 July 2007

Abstract

Adsorption of lead and copper ions by algae *Gelidium* and algal composite material was studied in a continuous stirred tank adsorber (CSTR). Danckwerts curves show that dead volumes and by-passes do not exist inside the reactor. The average residence time for cadmium ions was $\tau = 15.2 \pm 0.2$ min, and the useful adsorber volume $V_r = 540\,\text{cm}^3$.

Varying stirring velocity in the range 100–270 rpm the breakthrough curves show that a resistance to the mass transfer exists in the film of fluid around particles.

The analysis of the effect of the flow rate on the breakthrough curves leads to the conclusion that the curves sharpness increases with flow rate.

As expected, the larger the initial lead concentration, the faster the breakthrough of the metal, as the binding sites became more quickly saturated. The slope of the breakthrough curve increases when increasing the influent concentration.

For higher initial pH values, the breakthrough time increases since metal uptake capacity increases.

Biosorbents regeneration can be achieved by metal ions desorption with nitric acid as eluant. Desorption is an ion exchange process between metal ions loaded in the biomass and H^+ ions in the solution.

Two mass transfer models were developed to simulate biosorption and desorption performances. These models were able to predict the experimental results in a quite good manner.

Keywords: Biosorption; Lead(II); Copper(II); *Gelidium*; Algal composite material; Continuous adsorber

1. Introduction

New technologies involving the removal of metals ions from wastewaters have directed attention to biosorption based on metal binding capacities of various biological materials. Algae, bacteria, fungi and yeasts have proved to be potential metal biosorbents [1–4]. The major advantages of biosorption over conventional treatment methods include: low cost, high efficiency, minimization of chemical and or biological sludge, regeneration of biosorbent, and the possibility of metal recovery [1,2]. In order to apply these low-cost adsorbents in an industrial process, continuous flow studies need to be performed. There are three basic types of sorption contact systems: packed-bed and fluidized-bed columns, and completely mixed systems. The use of the first configuration has been widely investigated because theoretically it should be the most effective operating system [5–7]. However, it cannot handle suspension, requires column alternation, scales up by multiplying units and it is sensitive to pressure drop. An alternative way is a continuous stirred tank reactor (CSTR) configuration, which allows handling suspensions, makes possible the combination of flow schemes and does not need immobilization of the biomass to maintain the integrity of the adsorbent particles, if there is a biosorbent filtration step. Different studies have been performed in CSTR coupled with microfiltration and/or ultrafiltration system, for biomass recovery [8–13]. Particularly, Beolchini et al. [8] studied the biosorption of copper by *Arthrobacter* sp. in a UF/MF membrane reactor. Continuous biosorption of copper ions from dilute feed streams using magnetic weak-base anion exchangers in a CSTR was also studied by Dahlke et al. [14]. Menoud et al. [15] also studied the adsorption of Cu^{2+}, Ni^{2+}, Co^{2+} and Zn^{2+} by a chelating resin in a CSTR. Experiments were simulated by a global kinetic model comprising

---

* Corresponding author. Tel.: +351 225081669; fax: +351 225081449.
E-mail addresses: vilar@fe.up.pt (V.J.P. Vilar), cbotelho@fe.up.pt (C.M.S. Botelho), bventura@fe.up.pt (R.A.R. Boaventura).

1385-8947/$ – see front matter © 2007 Elsevier B.V. All rights reserved.
doi:10.1016/j.cej.2007.07.059

Nomenclature

a_p	specific surface area for thin plates particles
C_b	metal concentration in the bulk (mg l^{-1} or mmol l^{-1})
C'_b	proton concentration in the bulk (mmol l^{-1})
C_{b_0}	initial metal concentration in the bulk (mg l^{-1} or mmol l^{-1})
C'_{b_0}	initial proton concentration in the bulk (mmol l^{-1})
C_E	feed concentration (mg l^{-1} or mmol l^{-1})
C_f	metal concentration in the film (mg l^{-1} or mmol l^{-1})
C_{final}	metal concentration in the solution at the end of the saturation or elution process (mg l^{-1} or mmol l^{-1})
C_H	equilibrium concentration of proton in the fluid phase (mmol l^{-1})
C_M	equilibrium concentration of metal in the fluid phase (mmol l^{-1})
C_T	total (metal + acid) liquid concentration (mmol l^{-1})
C_{T_E}	total feed (acid) liquid concentration (mmol l^{-1})
C_{T_0}	initial total (metal + acid) liquid concentration (mmol l^{-1})
C_0	initial cadmium concentration in the adsorber after the step input (mmol l^{-1})
d_p	particle diameter (cm)
D_h	homogeneous diffusion coefficient (cm^2 s^{-1})
D_m	molecular diffusivity of the metal ion in solution (cm^2 s^{-1})
k_f	film mass transfer coefficient (cm s^{-1})
k_p	mass transfer coefficient for intraparticle diffusion (cm s^{-1})
K_H	equilibrium proton constant (l mmol^{-1})
K_L	equilibrium constant of Langmuir (l^{-1} mg)
K_M	equilibrium metal constant (l mmol^{-1})
K_H^M	selectivity coefficient between ion M in the particle and H in solution
N_d	number of mass transfer units by intraparticle diffusion
N_f	number of mass transfer units by film diffusion
pH_{AE}	final pH of interstitial fluid inside the adsorber
pH_{AI}	initial pH of interstitial fluid inside the adsorber
pH_{SE}	pH of feed solution
$\langle q \rangle$	average metal concentration in the solid phase (mg g^{-1} or mmol g^{-1})
q_E	solid phase concentration in equilibrium with C_E (mg g^{-1} or mmol g^{-1})
q_H	equilibrium concentration of proton in the biomass (mg g^{-1} or mmol g^{-1})
q_M	equilibrium concentration of metal in the biomass (mg g^{-1} or mmol g^{-1})
q_{M_0}	metal concentration in the solid phase after biomass saturation (mg g^{-1} or mmol g^{-1})
q^*	solid phase concentration in equilibrium with C_f (mg g^{-1} or mmol g^{-1})
Q	flow rate (cm^3 min^{-1})
Q_{max}	concentration of carboxylic groups or maximum capacity of biomass (mg g^{-1} or mmol g^{-1})
R	half of thickness of the thin plate (cm)
Sh	Sherwood number
t	time (s)
T	temperature (°C)
V_r	adsorber volume capacity (cm^3)
$\langle y \rangle$	dimensionless average concentration in the solid phase
y_b	dimensionless concentration in the fluid phase
y_f	dimensionless concentration in the fluid phase at the film
y_T	dimensionless total concentration in the fluid phase
y^*	dimensionless concentration in the solid phase at the particle surface
W	mass of biosorbent (g)

Greek symbols

ε	adsorber porosity
θ	dimensionless time
ρ_{ap}	apparent density of particles (g cm^{-3})
τ	space time (s)
τ_d	time constant for intraparticle diffusion
τ_f	time constant for film diffusion
ξ	adsorber capacity factor for saturation
ξ'	adsorber capacity factor for desorption

mass transfer in a liquid film around the resin particles, with diffusion through the pores and reaction on the adsorption sites. Kinetics has been found to be limited by film mass transfer for all metals studied, and the equilibrium given by the Langmuir equation.

In this work, biosorption of lead and copper ions will be studied in a “Carberry” type adsorber packed with algae *Gelidium* and composite material particles, continuously feed with the metal ions solution. The effects of the initial inlet concentration, flow rate, initial pH and stirring velocity on the breakthrough curves were investigated. Regeneration studies were also performed. Mass transfer models for saturation and elution processes were developed to simulate the breakthrough curves at different initial conditions.

2. Materials and methods

2.1. Biosorbents

An algal waste from agar extraction industry was immobilized with an organic polymer (polyacrylonitrile, PAN) and used in this study as well as algae *Gelidium*, which is the raw material for agar extraction. The characteristics and preparation of both materials were presented in a previous work [16,17]. Additional information on this issue is given in supplementary data.

2.2. Copper, lead and cadmium solutions

Copper(II), lead(II) and cadmium(II) solutions were prepared by dissolving a weighed quantity of copper(II) chloride dehydrate (Riedel-de-Haën, purity > 99%), anhydrous $PbCl_2$ (Merck-Schuchardt, purity > 98%) and cadmium(II) chloride dehydrate (Sigma–Aldrich > 99%) in distilled water. Before adsorption in the continuous column system, the pH of each test solution was adjusted to the required value with diluted HNO_3 and NaOH solutions.

2.3. Adsorber continuous experiments

CSTR experiments were conducted in a "Carberry" or hampers adsorber. The hampers were packed with algae *Gelidium* or composite material. Perfect mixing was ensured by a mechanical stirrer. An acrylic jacket surrounding the adsorber body allowed for temperature control. The apparent densities of the biosorbents determined by mercury intrusion (PORESIZER 9320) were 1.34 and 0.25 g cm^{-3}, respectively, for algae *Gelidium* and the composite material [18].

A known quantity of algae *Gelidium* or composite material (≈10 g) was placed in the hampers. The solution was pumped through the CSTR at a flow rate of 35.5 ml min^{-1} by a peristaltic pump (Ismatec Ecoline VC-380). The flow rate was measured several times during the experiment. CSTR effluent samples were collected regularly and analysed by Atomic Absorption Spectrophotometer (GBC 932 Plus AAS). The effluent pH was not controlled, but it was continuously monitored.

At the end of the sorption process, the metal loaded biomass was regenerated using 0.1 M HNO_3. The procedures for collection and analysis of the elution outlet samples were the same used in the sorption protocol. After elution, the bed was washed with distilled water until the effluent pH reached water pH. The regenerated biomass was dried in the oven, at 50 °C, during two days. The adsorber was washed with nitric acid (20%) and distilled water to remove contaminations.

3. Theoretical approach

3.1. Equilibrium adsorption model

A mathematical equilibrium model has been developed assuming that only one kind of active sites (carboxylic groups) is present in the biosorbent cell walls [19], which are responsible for metal biosorption at pH < 7.0, and for competition between metal ions and H^+. The model is based on the apparent equilibrium binding constants, K_H and K_M for H^+ and M^{2+}, respectively. The total metal uptake can be calculated as [19]:

$$q_M = \frac{Q_{max} K_M C_M}{1 + K_H C_H + K_M C_M} \tag{1}$$

This equation can be converted in the Langmuir equation dividing by $1 + K_H C_H$,

$$q_M = \frac{Q_{max} K_L C_M}{1 + K_L C_M} \tag{2}$$

where

$$K_L = \frac{K_M}{1 + K_H C_H} \tag{3}$$

From K_M, K_H values it is possible to calculate the Langmuir equilibrium constant for each pH.

3.2. Equilibrium desorption model

Desorption was considered as an ion exchange process, in which metal ions are released into the solution by exchange with H^+ with a 1:1 stoichiometry exchange. Equilibrium desorption was well described by the mass action law [20]:

$$q^* = \frac{K_H^M Q_{max} C_b}{C_T + (K_H^M - 1) C_b} \tag{4}$$

where K_H^M and Q_{max} values have been obtained by desorption equilibrium studies and potentiometric titrations experiments [20], respectively, resulting the following values: 0.93 ± 0.07 and 1.1 ± 0.3, and 0.36 ± 0.01 and 0.16 ± 0.01 mmol g^{-1}, respectively, for algae *Gelidium* and composite material.

3.3. CSTR modelling

Mass balance equations for the saturation and elution processes have been developed in order to predict the metal ions concentration profiles as a time function.

3.3.1. Saturation

A model was developed with the following assumptions: isothermal operation, adsorption equilibrium described by the Langmuir isotherm, external (film) resistance to mass transfer and internal mass transfer resistance described by the LDF approximation. The model equations in the dimensionless form are:

Mass conservation in the fluid around particles

$$\frac{dy_b}{d\theta} = 1 - y_b - \xi \frac{d\langle y \rangle}{d\theta} \tag{5}$$

Mass conservation inside particles (linear driving force, LDF)

$$\frac{d\langle y \rangle}{d\theta} = \frac{N_f}{\xi}(y_b - y_f) \tag{6}$$

Mass conservation in the fluid film surrounding the particles

$$\frac{d\langle y \rangle}{d\theta} = N_d(y^* - \langle y \rangle) \tag{7}$$

Initial conditions can be described as,

$$\theta = 0, \quad y_b = 0, \quad y_f = 0, \quad \langle y \rangle = 0 \tag{8}$$

3.3.2. Elution

An elution model was developed with the following assumptions: isothermal operation, adsorption equilibrium described by the mass action law and internal mass transfer resistance described by the LDF approximation. All concentrations are expressed in mmol l^{-1}.

Mass conservation in the fluid around particles

$$\frac{dy'_b}{d\theta} = -y'_b - \xi' \frac{d\langle y\rangle}{d\theta} \tag{9}$$

Total mass conservation in the fluid around particles

$$\frac{dy_T}{d\theta} = \frac{C_{T_E}}{C_{T_0}} - y_T \tag{10}$$

Initial conditions:

$$\theta = 0, \quad y'_b = \frac{C_{b_0}}{C_{T_0}}, \quad y_T = 1, \quad \langle y\rangle = \frac{q_M}{Q_{max}} \tag{11}$$

Resolution of equations models was solved by LSODA subroutine [21]. A more detailed description of mass transfer models is given in supplementary data.

4. Results and discussion

The model parameters for Eq. (1) obtained for lead biosorption are [19]: $Q_{max} = 0.26 \pm 0.01$ and 0.096 ± 0.003 mmol g^{-1}, $pK_H = \log K_H = 3.92 \pm 0.07$ and 4.7 ± 0.1, and $pK_M = \log K_M = 4.02 \pm 0.06$ and 4.6 ± 0.1, respectively, for algae *Gelidium* and composite material. For copper biosorption are [22]: $Q_{max} = 0.49 \pm 0.02$ and 0.177 ± 0.009 mmol g^{-1}, $pK_H = \log K_H = 4.3 \pm 0.1$ and 4.7 ± 0.1, and $pK_M = \log K_M = 3.1 \pm 0.1$ and 3.5 ± 0.1, respectively, for algae *Gelidium* and composite material.

4.1. Effect of stirring rate

The well mixed adsorber hydrodynamic conditions (stirring velocity and flow rate) were selected from experiments with Cd(II) in the absence of biosorbent, and with Cu(II) in the presence of algae *Gelidium*, at three difference stirring rates. The system response to a step inlet cadmium concentration of 22.2 mg l^{-1} was studied in the first experiment. The system response to an input of distilled water was also studied at a 35.5 cm^3 min^{-1} flow rate and 270 rpm stirring velocity (see supplementary data).

For a step input of solute (cadmium solution), the mass balance to the CSTR, without biosorbent, leads to:

$$QC_E = QC_b + \varepsilon V_r \frac{dC_b}{dt} \tag{12}$$

Integrating Eq. (12) for $t = 0$ and $C_b = 0$; $t = t$ and $C_b = C_b$, gives:

$$F(t) = 1 - \exp\left(-\frac{1}{\tau}t\right) \quad \text{or} \quad \ln[1 - F(t)] = -\frac{1}{\tau}t \tag{13}$$

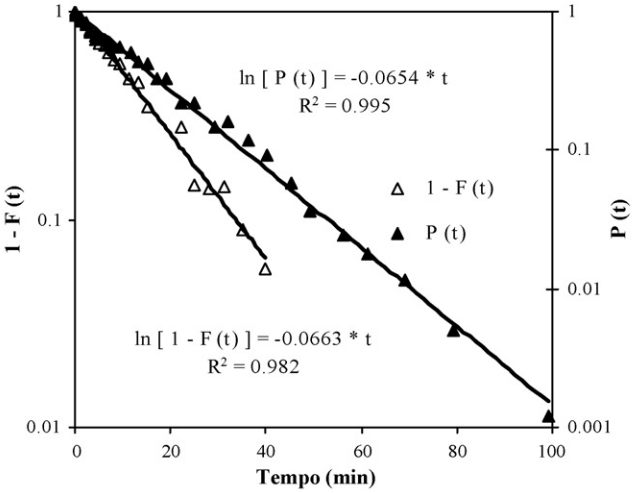

Fig. 1. Linearized responses to an inlet step of cadmium solution ($C_E = 22.2$ mg l^{-1}) and to an inlet purge of distilled water.

where $F(t) = C_b/C_E$ is the Danckwerts curve, or, the adsorber normalized response to a step input of solute in concentration C_E.

For a purge input, we get:

$$0 = QC_b + V_r \frac{dC_b}{dt} \tag{14}$$

Integrating Eq. (14) for $t = 0$ and $C_b = C_0$; $t = t$ and $C_b = C_b$, leads to:

$$P(t) = \exp\left(-\frac{1}{\tau}t\right) \quad \text{or} \quad \ln[P(t)] = -\frac{1}{\tau}t \tag{15}$$

where $P(t) = C_b/C_0 = 1 - F(t)$ is the adsorber normalized response to a purge input ($C_E = 0$) and C_0 is the initial cadmium concentration in the adsorber after the step input.

Representing the logarithm of $1 - F(t)$ and $P(t)$ as time functions, two straight lines with negative slopes were obtained, as observed in Fig. 1. This indicates perfect agitation conditions within the adsorber, without dead volumes or by-passes. So, the mean residence time is equal to the space time (τ), which can be determined by the straight line slopes: $\tau = 15.1 \pm 0.3$ and 15.3 ± 0.2 min. From the average value, $\tau = 15.2 \pm 0.2$ min, the useful volume of the adsorber, $V_r = 540$ cm^3 is obtained.

Fig. 2 shows that even at the highest stirring rate (270 rpm), the external (film) mass transfer was not eliminated, and the breakthrough curves for stirring velocities of 180 and 270 rpm overlap, which means that the mass resistance in the film remains constant. So, higher stirring rates are needed to eliminate the film resistance. This situation was not studied due to the system limitations (stability problems with the adsorber). So, the studies were conducted in the limit conditions of stirring allowed by the equipment.

Additional resistances due to the hampers and the high solid compacting inside them also exist.

In order to describe the experimental results, a mass transfer model was developed, including a mass transfer resistance in the film and particles, where equilibrium between metal concentration in the solid phase and solution is given by

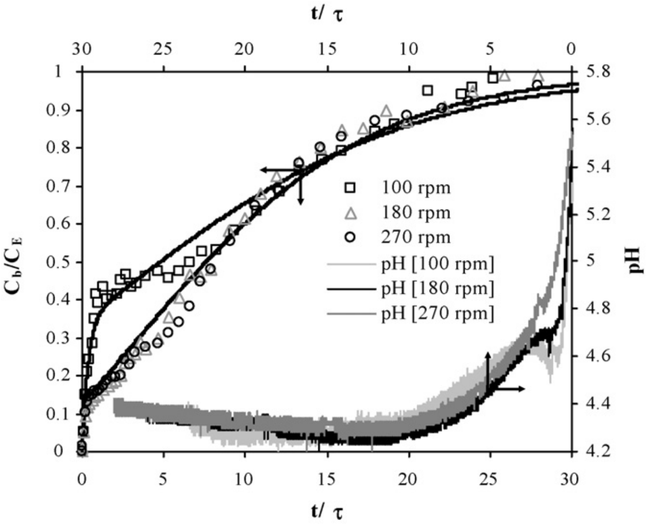

Fig. 2. Experimental data and simulated concentration profiles for Cu^{2+} continuous biosorption onto algae *Gelidium*: 100, 180 and 270 rpm.

the Langmuir isotherm. Table 1 presents the main parameters used in the model simulation. The intraparticle diffusion coefficient, D_h, was determined by batch dynamic studies at different pH (5.3, 4 and 3) [22]. The average D_h for Cu^{2+} is 3.2×10^{-8} and 2.3×10^{-8} $cm^2\,s^{-1}$ and for Pb^{2+} is 3.7×10^{-8} and 2.5×10^{-8} $cm^2\,s^{-1}$, respectively, for algae and composite material. The film coefficient, k_f, has been regressed from the experimental breakthrough curves, by minimizing the sum of the squared deviations between experimental and predicted values. Equilibrium Langmuir constants were determined by the discrete model (Eq. (1)), for the equilibrium pH inside the column, considered as the final pH value (Fig. 2).

Fig. 2 compares the experimental and simulated breakthrough curves. Simulation is better if Q_{max} is increased around 40%, suggesting that the binding capacity of Cu^{2+} in the CSTR is higher than that obtained in the batch system (see supplementary data). So, equilibrium is underestimated. The uptake capacity obtained was ≈12.3 mg Cu^{2+} g^{-1} of algae, two times higher than the obtained by the Langmuir equation (5.9 mg Cu^{2+} g^{-1}) for an equilibrium pH of 4.3.

Biosorption of metal ions by algae *Gelidium* is accomplished by the release of H^+, K^+, Na^+, Ca^{2+}, Mg^{2+} and others ions, due the ion exchange mechanism. About 30% of copper ions are adsorbed by ion exchange with H^+.

In a batch system, desorption of organic matter from the surface of the biosorbent to the solution occurs, until equilibrium between the organic carbon concentration in solution and at the surface is reached. An amount of 13 mg of organic carbon is released to the solution, per gram of biosorbent, which competes with particles surface to bound metal ions, decreasing the biosorption capacity. The interaction of dissolved organic matter with metal ions has been studied by several authors [23,24]. Benedetti et al. concluded that 50% of Cd and 99.99% of Cu bounds to dissolved organic matter containing fulvic and humic acids [25]. Grassi et al. [23] verified that the adsorption of Cu^{2+} onto modified Al_2O_3 decreased as the dissolved organic matter commercial humic acid increased and was maximal in the neutral pH range, and decreased at either low or high pH values. Wang et al. [26] studied the adsorption of Cd^{2+}, Co^{2+}, Cr^{3+}, Cu^{2+}, Ni^{2+}, Pb^{2+} and Zn^{2+} ions in secondary sludge samples collected from the Back River Wastewater Treatment Plant, Baltimore. They observed that in the alkaline pH region, the uptake of Cu^{2+}, Ni^{2+} and Co^{2+} decreases with the pH increase, primarily due to the high dissolved organic matter concentrations in high pH conditions. Results also showed that under neutral and low pH conditions, the dissolved organic matter effects on metal uptake are insignificant.

The biosorbents used in continuous experiments were previously suspended in distilled water, and submitted to vacuum under agitation, in order to remove the air from pores and the organic matter easily desorbed. Moreover, the compacted adsorber with biosorbent was washed with distilled water during 2 h, before the experiment. Using these pre-treatments, the concentration of dissolved organic matter in solution is low and does not interfere in the adsorption process. The uptake capacities, determined for algae *Gelidium* in batch system can be underes-

Table 1
Mass transfer parameters for copper biosorption at different operation conditions

	K_M ($l\,mg^{-1}$)	Q_{max} ($mg\,g^{-1}$)	ξ	ε	k_p ($cm\,s^{-1}$)	$k_p a_p$ (min^{-1})	D_h ($cm^2\,s^{-1}$)	k_f ($cm\,s^{-1}$)	N_d	ξN_d	N_f
rpm											
100	0.010	44	7.75	0.986	1.9×10^{-5}	0.23	3.2×10^{-8}	7.0×10^{-4}	3.5	26.8	1.8
180 and 270	0.010	44	7.65	0.987	1.9×10^{-5}	0.23	3.2×10^{-8}	3.0×10^{-3}	3.5	26.5	7.3
Q ($ml\,min^{-1}$)											
24	0.019	11.2	2.7	0.926	3.6×10^{-5}	0.43	6.0×10^{-8}	6.0×10^{-3}	9.0	25.3	120.8
35.5	0.017	11.2	2.7	0.926	3.6×10^{-5}	0.43	6.0×10^{-8}	5.0×10^{-3}	6.1	17.1	67.9
pH_{AE}											
5.2	0.15	16	10.5	0.917	1.5×10^{-5}	0.18	2.5×10^{-8}	1.0×10^{-3}	2.5	27.3	15.1
4.1	0.04	20	8.8	0.924	1.5×10^{-5}	0.18	2.5×10^{-8}	8.0×10^{-4}	2.5	22.3	11.1
C_E ($mg\,l^{-1}$)											
25.2[a]	0.16	53.9	40.0	0.983	2.2×10^{-5}	0.27	3.7×10^{-8}	6.0×10^{-3}	4.0	159.4	18.7
9.5[b]	0.15	20	19.7	0.940	2.2×10^{-5}	0.27	2.5×10^{-8}	2.0×10^{-3}	2.6	51.2	21.6
25.6[b]	0.15	16	10.5	0.917	1.5×10^{-5}	0.18	2.5×10^{-8}	1.0×10^{-3}	2.5	27.3	15.1

[a] Gelidium.
[b] Composite material.

timated, due metal ions competition between dissolved organic matter and surfaces. For the composite material, only a low concentration of organic matter is released to the solution, therefore, the same adsorption capacity was obtained for continuous and batch systems.

Associated errors to equilibrium parameters determination, as pH change inside the adsorber (it was considered the final pH of the experiment to determine the equilibrium parameters by the discrete model) and algae *Gelidium* heterogeneity (the algae was harvested in different seasons and sites), can also contribute to different uptake capacities obtained in batch and continuous systems.

The film mass transfer coefficient, k_f, can be obtained from the "knee" of the breakthrough curve (Fig. 2). The "knee" height for the 100 rpm experiment corresponds to $C_b/C_E \approx 0.42$ whereas for experiments at 180 or 270 rpm $C_b/C_E \approx 0.14$, which means a higher mass transfer resistance in the film for lower stirring velocities. Simulated curves for three different values of k_f confirm that decreasing k_f (increasing the film resistance) the "knee" height increases (see supplementary data).

The external mass transfer resistance is proportional to the thickness of the stationary fluid layer surrounding the particles, which is controlled by the stirring rate of the bulk solution. A higher stirring rate reduces the film thickness and should eventually eliminate the film resistance.

The film mass transfer resistance can be estimated by the Sherwood number ($Sh = k_f d_p/D_m$), that is equal to 2 for isolated spherical particles, in the absence of stirring [27]. Considering Cu^{2+} diffusion coefficient in aqueous solution, $D_m = 7.2 \times 10^{-6}\,\mathrm{cm\,s^{-1}}$ [28] and $Sh = 2$, k_f is equal to $1.4 \times 10^{-3}\,\mathrm{cm\,s^{-1}}$ for algae *Gelidium* (thickness = 0.1 mm). This value is approximately two times lower than the obtained for 180 and 270 rpm stirring rates. The k_f value for 100 rpm stirring rate is half of the estimated in the absence of stirring, suggesting the presence of other resistances, as those of the hampers mesh, the compacting bed of algae or the thin plate geometry of the particles.

Table 1 presents the indicators for the mass transfer resistance in the film and in particles N_f and ξN_d, respectively. $N_f < \xi N_d$ indicates that the film resistance is higher than the particle resistance, which means that diffusion in the film is the limitant step in the biosorption process.

4.2. Effect of flow rate

In order to study the flow rate influence on the biosorption process, two copper biosorption experiments were performed using the composite material, at 35.5 and 24.0 $\mathrm{cm^3\,min^{-1}}$ flow rates. Increasing the flow rate, the time residence in the adsorber decreases, increasing the superficial velocity inside and the sharpness of the breakthrough curves (see supplementary data). Representing the breakthrough curves as a function of the dimensionless time (Fig. 3), it can be seen that the two curves converge, suggesting that the flow rate influence on the biosorption process only affects the time needed to reach equilibrium. The same copper uptake was obtained from the two experiments (0.64 mmol Cu^{2+} $\mathrm{g^{-1}}$ composite material), and 0.21 mmol H^+ was released to the solution (≈32% of the adsorbed copper ions). In this case, the mass transfer model fits well the experimental results, as it can be seen in Fig. 3.

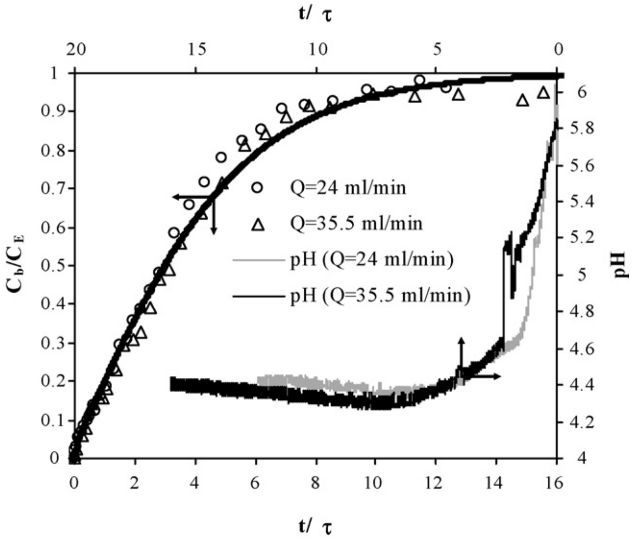

Fig. 3. Experimental data and simulated concentration profiles for Cu^{2+} continuous biosorption onto composite material, at two different flow rates.

At higher flow rates, low film resistances and higher k_f values are obtained. The lowest resistance to film diffusion was found for the composite material, due to the low particles compaction inside the hampers. N_f values higher than ξN_d values were found for the composite material, suggesting that the process is intraparticle mass transfer controlled (see Table 1).

A k_f value of $1.6 \times 10^{-6}\,\mathrm{cm\,s^{-1}}$ was estimated in the absence of stirring ($Sh = 2.0$), for an average particles diameter of 0.9 mm (composite material), which is around 30 times lower than the k_f value obtained from the simulated curves. This result suggests that, despite the existence of a film mass transfer resistance, it has been highly reduced by stirring. The reduction is higher for the composite material than for algae *Gelidium*, maybe due to the particles geometry and bed compaction, which turns the binding sites more accessible.

4.3. Effect of the initial concentration

The influence of the inlet concentration in the biosorption process, using a CSTR adsorber, was studied for lead biosorption by the composite material. The initial lead concentration has a significant effect on the breakthrough curves as illustrated in Fig. 4. As expected, higher the initial lead concentration, faster the metal breakthrough, since the binding sites became quickly saturated. The lead uptake capacity, achieved in both experiments, was approximately 12 mg Pb^{2+} $\mathrm{g^{-1}}$ composite material.

For $C_E = 25.6\,\mathrm{mg\,l^{-1}}$ adsorbed metal does not reach the maximum uptake capacity of the adsorbent (for $Q_{max} = 20\,\mathrm{mg\,g^{-1}}$, the lead uptake capacity in equilibrium was only $15.9\,\mathrm{mg\,g^{-1}}$), which means that there was not enough time to saturate the biosorbent. Decreasing the value of Q_{max} for $16.0\,\mathrm{mg\,g^{-1}}$ (the lead uptake capacity in equilibrium with $C_E = 25.6\,\mathrm{mg\,l^{-1}}$ is

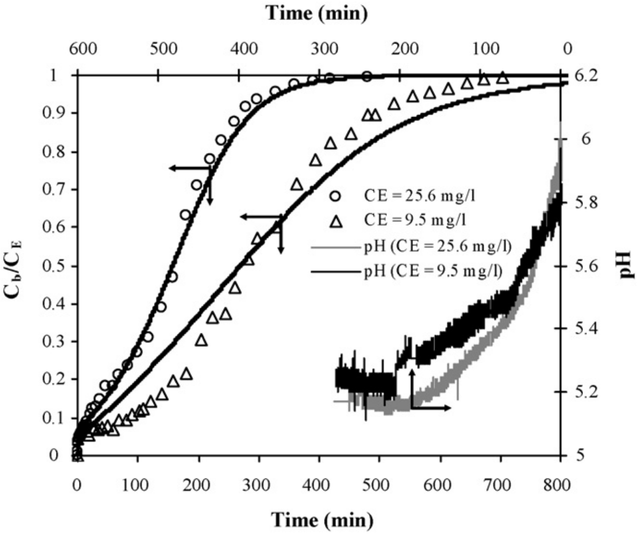

Fig. 4. Experimental data and simulated concentration profiles for continuous Pb^{2+} biosorption onto composite material, at two different inlet concentrations.

12.7 mg g^{-1}), a better description of the experimental results is obtained (Table 1).

For $C_E = 9.5\ mg\ l^{-1}$ the initial part of the experimental curve shows a little “knee”, due to the resistance to mass transfer in the film (Fig. 4). Results suggest that, due to high Pb^{2+} diffusivity in particles, the ions fed to the adsorber are immediately adsorbed. For higher Q_{max} a better description of the experimental results by the model is obtained, but with adsorption capacities higher than those obtained in equilibrium.

Biosorption of Pb^{2+} on alga *Gelidium* was also performed (see supplementary data). The uptake capacity of alga *Gelidium* was 36.4 mg Pb^{2+} g^{-1} (pH_{AE} 4.8). The simulated curve does not fit the experimental results using the value of Q_{max} determined by the Langmuir isotherm (54 mg g^{-1}). Increasing this value to 82 mg g^{-1}, the curve has a translation in the positive axis of time, but still continues not fitting the experimental data. Increasing K_M to 0.161 mg^{-1}, the mathematic model better describes the experimental results, as in the initial part of the curve the active sites with higher affinity to the metal ions are the occupied ones. In the discrete model are only used the medium affinity to the active sites. Considering the continuous model, $K_{Pb} = 0.161\ mg^{-1}$ is inside of the interval of the carboxylic affinity constants, considering a continuous equilibrium model [19]. It can be concluded that, in the biosorption of Cu^{2+} as in the biosorption of Pb^{2+}, the equilibrium data cannot be used in the CSTR biosorption.

4.4. Effect of the initial pH

The solution pH plays an important role in metal ion adsorption, as it was already concluded from equilibrium and kinetic experiments in batch systems [19,29,30]. In order to study the pH effect on lead biosorption onto the composite material, in a CSTR adsorber, two experiments were performed at different pH inlet solutions (pH_{SE} 5.4 and 4.4; pH_{AI} 6.0 and 4.0, which corresponds to pH_{AE} 5.2 and 4.1 in the equilibrium).

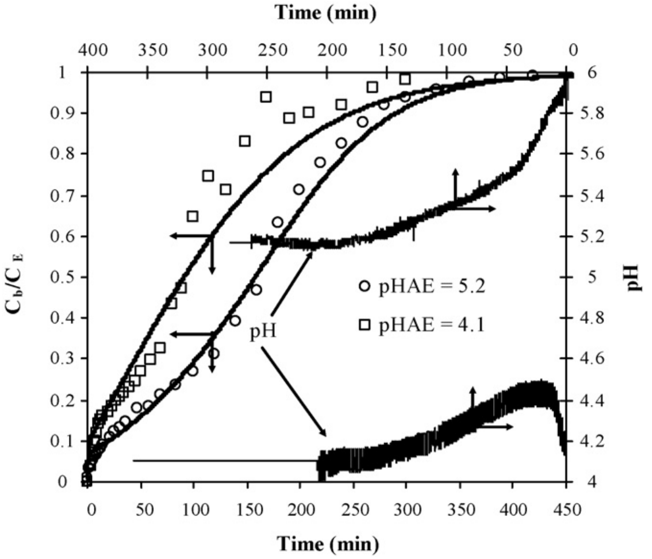

Fig. 5. Experimental data and simulated concentration profiles for continuous Pb^{2+} biosorption onto composite material, at two different initial pH.

The concentration profiles represented in Fig. 5 result from ion exchange between metal (solution) and H^+ (solid). As H^+ is released to the solution, the solution pH decreases. For pH_{SE} 4.4, the effluent pH is constant, due to the high proton concentration and the competition with metal ions. For higher pH values more time is needed to reach biomass saturation, since the uptake capacity also increases.

Mass transfer parameters for both experiments are presented in Table 1. The film resistance increases when decreasing the pH, as observed in Fig. 5, through the height of the curve initial “knee”. Due to competition with H^+, the electrostatic adsorption binding force decreases with pH, increasing the film resistance.

4.5. Regeneration studies

After the biosorbents saturation with lead ions, the regeneration process has been studied using HNO_3 as eluant. Fig. 6 shows that Pb^{2+} desorption is complete (≈451 and 100 mg Pb^{2+} were released into solution, respectively, for algae and composite material). The same results were obtained for lead and copper desorption in a continuous packed-bed column [22].

In the batch system, Cu^{2+} elution was about 80%, for the composite material and, around, 95% for the alga *Gelidium* [20], whereas complete desorption (100%) was obtained in the continuous system (CSTR). Desorption is very fast ($t = 3\tau$) and maximum concentrations of 600 and 150 mg l^{-1} were achieved, respectively, for alga and composite material. The solid–liquid ratio (*S*/*L*, g l^{-1}) is 23.4 and 15.7 and the concentration factor (CR) is 23.8 and 15.8, respectively, for alga and composite material.

When the desorption process is 100% efficient, CR can be estimated from [20]:

$$CR = \left(\frac{S}{L}\right) \frac{Q_{max} K_L}{1 + K_L C_{final}(\text{adsorption})} \qquad (16)$$

Table 2
Mass transfer parameters for lead elution

Biosorbent	K_H^{Pb}	Q_{max} (mmol g^{-1})	ξ'	ε	k_p (cm s^{-1})	$k_p a_p$ (min^{-1})	D_h (cm^2 s^{-1})	N_d	$\xi' N_d$
Gelidium	0.16	0.36	41.5	0.983	3.3×10^{-5}	0.4	5.5×10^{-8}	5.9	245
Composite material	1.1	0.16	21.7	0.917	1.1×10^{-4}	1.3	1.8×10^{-7}	18.6	403

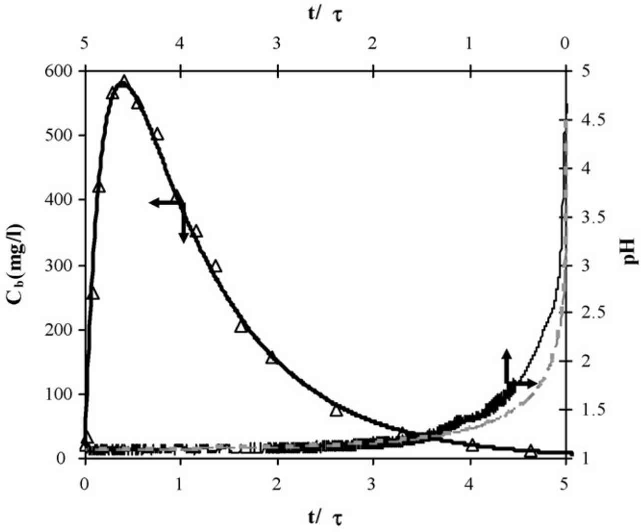

Fig. 6. Experimental data and simulated concentration profiles for continuous Pb^{2+} elution onto composite material.

CR values predicted by Eq. (16) using the equilibrium data are 26.6 and 19.3, respectively, for experiments 5 and 9 (using C_{final} values from Table 1, in supplementary data, and equilibrium parameters from Table 2), which means that the concentration factor can be estimated from equilibrium data.

Table 2 presents model parameters used in the elution mass transfer model. The breakthrough curves are well predicted by the model, as it can be seen in Fig. 6 (see supplementary data). In the simulation, it was assumed that the selectivity coefficient for Pb^{2+} ($K_H^M = K_H^{Pb}$) is equal to that obtained for Cu^{2+} in the batch system. For $K_H^{Pb} = 0.93$, the maximum lead concentration obtained from the model simulation is lower than the experimentally obtained. If $K_H^{Pb} = 0.16$, the simulated curve fits well the experimental data. The difference can be attributed to the greater standard errors associated with the measurements of high metal concentrations, and to the selected value for Pb^{2+} selectivity.

From $\xi' N_d$ values (Table 2), it can be concluded that the mass transfer resistance in the particle is very small, due to the fast diffusion of Pb^{2+} from the biomass surface into the solution, by ion exchange with H^+. Fig. 6 shows that pH decreases rapidly to the inlet value. The simulated curve also corresponds well to the experimental pH profile, and confirms that, in this system, elution is an ion exchange process.

5. Conclusions

The present study shows that algae *Gelidium* and algal composite material are an effective biosorbents for the adsorption of copper and lead ions from aqueous solution in a CSTR. The film resistance is higher for lower stirring velocities, increasing the "knee" of the initial part of the breakthrough curve, and for the higher stirring velocity this resistance was not eliminated. The flow rate only affected the time necessary to saturate the biosorbent. A higher initial metal concentration decreases the metal breakthrough time, since the binding sites become quickly saturated. Increasing the initial pH, more deprotonated sites are available, increasing the uptake capacity and the saturation time. The biosorbents can be reutilized in a fast way by using a concentrated acid solution in a fast way. The mass transfer model for adsorption and desorption processes can be used to describe the experimental results, however it could be seen that the equilibrium data are underestimated in some situations due principally to the competition of organic matter in solution.

Acknowledgements

Financial support by FCT and European community through FEDER (project POCI/AMB/57616/2004) is gratefully acknowledged. The authors are grateful to FCT for V. Vilar's doctorate scholarship (SFRH/BD/7054/2001).

Appendix A. Supplementary data

Supplementary data associated with this article can be found, in the online version, at doi:10.1016/j.cej.2007.07.059.

References

[1] J. Wase, C. Forster, Biosorbents for Metal Ions, Taylor & Francis, London, 1997.

[2] B. Volesky, Biosorption of Heavy Metals, CRC Press, Montreal, 1990.

[3] B. Volesky, Sorption and Biosorption, first ed., BV Sorbex, Inc., Quebec, 2003.

[4] Y.S. Wong, N.F.Y. Tam, Wastewater Treatment with Algae, Springer, New York, 1998.

[5] M.M. Figueira, B. Volesky, K. Azarian, V.S.T. Ciminelli, Biosorption column performance with a metal mixture, Environ. Sci. Technol. 34 (2000) 4320–4326.

[6] P. Kaewsarn, Biosorption of copper(II) from aqueous solutions by pretreated biomass of marine algae *Padina* sp., Chemosphere 47 (10) (2002) 1081–1085.

[7] D.C.K. Ko, J.F. Porter, G. McKAY, Film-pore diffusion model for the fixed-bed sorption of copper and cadmium ions onto bone char, Water Res. 35 (16) (2001) 3876–3886.

[8] F. Beolchini, F. Pagnanelli, F. Vegliò, Modeling of copper biosorption by *Arthrobacter* sp. in a UF/MF membrane reactor, Environ. Sci. Technol. 35 (2001) 3048–3054.

[9] F. Beolchini, F. Pagnanelli, L. Toro, F. Vegliò, Continuous biosorption of copper and lead in single and binary systems using *Sphaerotilus natans* cells confined by a membrane: experimental validation of dynamic models, Hydrometallurgy 76 (2005) 73–85.

[10] F. Beolchini, F. Pagnanelli, L. Toro, F. Vegliò, Copper biosorption by *Sphaerotilus natans* confined in UF membrane module: experimental study and kinetic modelling, Hydrometallurgy 72 (2004) 21–30.

[11] F. Pagnanelli, F. Beolchini, A.D. Biase, F. Vegliò, Biosorption of binary heavy metal systems onto *Sphaerotilus natans* cells confined in an UF/MF membrane reactor: dynamic simulations by different Langmuir-type competitive models, Water Res. 38 (2004) 1055–1061.

[12] D. Barba, F. Beolchini, F. Vegliò, A simulation study on biosorption of heavy metals by confined biomass in UF/MF membrane reactors, Hydrometallurgy 59 (2001) 89–99.

[13] Z. Reddad, C. Gérente, Y. Andrès, J.-F. Thibault, P.L. Cloirec, Cadmium and lead adsorption by a natural polysaccharide in MF membrane reactor: experimental analysis and modelling, Water Res. 37 (2003) 3983–3991.

[14] T. Dahlke, Y.H. Chen, M. Franzreb, W.H. Holl, Continuous removal of copper ions from dilute feed streams using magnetic weak-base anion exchangers in a continuous stirred tank reactor (CSTR), React. Funct. Polym. 66 (10) (2006) 1062–1072.

[15] P. Menoud, L. Cavin, A. Renken, Modelling of heavy metals adsorption to a chelating resin in a fluidized bed reactor, Chem. Eng. Process 37 (1) (1998) 89–101.

[16] V.J.P. Vilar, C.M.S. Botelho, R.A.R. Boaventura, Equilibrium and kinetic modelling of Cd(II) biosorption by algae *Gelidium* and agar extraction algal waste, Water Res. 40 (2) (2006) 291–302.

[17] V.J.P. Vilar, F. Sebesta, C.M.S. Botelho, R.A.R. Boaventura, Equilibrium and kinetic modelling of Pb^{2+} biosorption by granulated agar extraction algal waste, Proc. Biochem. 40 (10) (2005) 3276–3284.

[18] V.J.P. Vilar, C.M.S. Botelho, R.A.R. Boaventura, Methylene blue adsorption by algal biomass based materials: biosorbents characterization and process behaviour, J. Hazard. Mater. 147 (2007) 120–132.

[19] V.J.P. Vilar, C.M.S. Botelho, R.A.R. Boaventura, Kinetics and equilibrium modelling of lead uptake by algae *Gelidium* and algal waste from agar extraction industry, J. Hazard. Mater. 143 (1–2) (2007) 396–408.

[20] V.J.P. Vilar, C.M.S. Botelho, R.A.R. Boaventura, Copper desorption from *Gelidium* algal biomass, Water Res. 41 (7) (2007) 1569–1579.

[21] A.C. Hindmarsh, Odepack, A Systematized Collection of Ode Solvers, in Scientific Computing, Scientific Computing, Amsterdam, 1983.

[22] V.J.P. Vilar, Uptake of metal ions in aqueous solution by algal waste from agar extraction industry, Ph.D. Thesis, Faculty of Engineering University of Porto, Porto, 2006.

[23] M.T. Grassi, B. Shi, H.E. Allen, Partition of copper between dissolved and particulate phases using aluminium oxide as an aquatic model phase: effects of pH, solids and organic matter, J. Braz. Chem. Soc. 11 (5) (2000) 516–524.

[24] A.Y.O. Matsuo, C.M. Wood, A.L. Val, Effects of copper and cadmium on ion transport and gill metal binding in the amazonian teleost tambaqui (*Colossoma macropomum*) in extremely soft water, Aquat. Toxicol. 74 (2005) 351–364.

[25] M.F. Benedetti, W.H.V. Riemsdijk, L.K. Koopal, D.G. Kinniburgh, D.C. Gooddy, C.J. Milne, Metal ion binding by natural organic matter: from the model to the field, Geochim. Cosmochim. Acta 60 (14) (1996) 2503–2513.

[26] J. Wang, C.P. Huang, H.E. Allen, Modeling heavy metal uptake by sludge particulates in the presence of dissolved organic matter, Water Res. 37 (2003) 4835–4842.

[27] D.M. Ruthven, Principles of Adsorption and Adsorption Processes, Wiley & Sons, New York, 1984.

[28] R.C. Reid, J.M. Prausnitz, B.E. Poling, The Properties of Gases & Liquids, fourth ed., McGraw-Hill Book Company, New York, 1987.

[29] V.J.P. Vilar, C.M.S. Botelho, R.A.R. Boaventura, Influence of pH, ionic strength and temperature on lead biosorption by *Gelidium* and agar extraction algal waste, Proc. Biochem. 40 (10) (2005) 3267–3275.

[30] V.J.P. Vilar, C.M.S. Botelho, R.A.R. Boaventura, Copper removal by algae *Gelidium*, agar extraction algal waste and granulated algal waste: kinetics and equilibrium, Bioresour. Technol. 99 (2008) 750–762.